International Journal of Grid and Distributed Computing
Vol. 9, No. 3 (2016), pp.91-98
http://dx.doi.org/10.14257/ijgdc.2016.9.3.11

Improvement of SVM Image Reconstruction Algorithm in ECT System

Li Yan[1*], Song Haifeng[1], Zhang Guangwu[1], Chen Deyun[1], Wang Zhao[2], Cui Peng[1]

[1.] School of Computer Science and Technology, Harbin University of Science and Technology, Harbin, 150080, China ;
[2.] Tax information centre of Harbin in Heilongjiang province,Harbin,150080,China
liyan@hrbust.edu.cn

Abstract

Due to the problem of low imaging accuracy and slow imaging speed when applying SVM image reconstruction algorithm in ECT system to dealing with a large amount of sample data set, the method of combining feature dimension reduction with SVM algorithm is proposed. This method classifies the sample data by using the way of clustering and extracts the feature parameter, finds out the connection between each sample and the feature, and deals the sample data with dimension reduction, thus finally getting the high-quality training sample. Then it trains the simplified sample data by applying SVM algorithm and obtains decision function, then the decision function is used to predict and image. The experimental results of image reconstruction show that this method greatly reduces the running time and improves the accuracy of imaging compared to using the SVM algorithm alone.

Keywords: *Electrical capacitance tomography; Support vector machine; Feature dimension reduction; image reconstruction*

1. Introduction

C Electrical Capacitance Tomography (ECT) [1,2] technique, as a kind of PT technique, appeared and developed in the late 1980s, possessing the advantages of non-invasive sensing, simple structure, low cost, fast reaction speed, high performance safety, wide-spread application, and so on [3,4]. However, owing to the limitations of the decrease in independent capacitance measurement values, the specialness of “soft field" in system sensitive field, and the non-linear features of problems remaining to be settled, it is difficult for the image reconstruction algorithm in ECT system to be realized, which is unable to satisfy the requirements of industrial application. So it becomes significant and urgent to put forward a better image reconstruction algorithm [5-8].

Because of its reliability and good generalization ability, Support Vector Machine (SVM) [9-14], as a hot spot of machine learning, is widely applied in many other areas, and also provides a favorable means to the image reconstruction in ECT system. But SVM has its own defects, among which the biggest defect is its slow training speed and low imaging accuracy when dealing with a large amount of sample data set. So this paper proposes a method of combining feature dimension reduction with SVM algorithm, or the FDRSVM algorithm for short, which efficiently solves the problems of long training time

ISSN: 2005-4262 IJGDC

and low imaging accuracy appearing in the course of applying SVM image reconstruction algorithm in ECT system to dealing with a large amount of sample data set.

2. Image Reconstruction Theory Based on SVM

2.1. The Basic Structure of ECT System

By measuring the capacitance value between the electrode pairs uniformly distributed on the surface of the pipe wall, and then by applying appropriate algorithm to reconstruct the spatial distribution of each phase flow inside the pipe wall, ECT system provides a feasible way to solve the problem of the parameters visualization measurement of the two-phase flow, even the parameter measurement of the multi-phase flow. A standard ECT system basically consists of three parts: the capacitance measurement sensor, the real-time data collection system and the image reconstruction display system. And it can also be divided into the following parts: uniformly distributed capacitance measuring sensor, data collection circuit, communication interface, embedded analysis system and image reconstruction display system, *etc*. The basic structure of ECT system is shown in Figure 1.

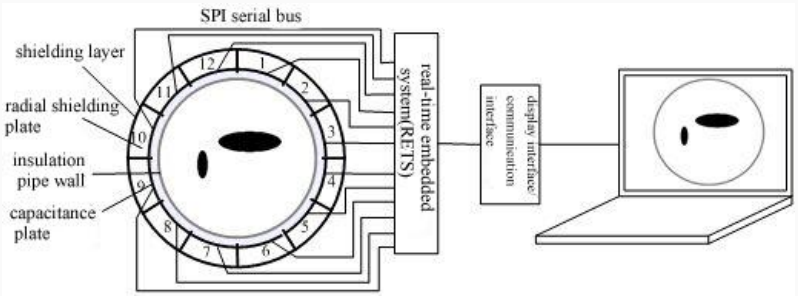

Figure 1. Basic Structure of ECT system

In ECT system, the capacitance measurement sensor basically consists of three parts: the circular insulation pipe wall, the measuring electrode uniformly distributed on the surface of insulation pipe wall and the shielding electrode used for shielding the measuring electrode. This kind of sensor possesses the advantages of high measuring sensitivity, excellent high-frequency performance and strong anti-interference ability, *etc*.

The medium concentration of each phase will change with the flow of multi-phase flow medium in the pipe. Because the medium's permittivity of each phase in the pipe are not the same, the measured capacitance value between the plates of measuring electrode will change with the changes of permittivity, and then the measuring sensor will transform the distribution of the multi-phase flow into the distribution of the measured output capacitance value.

The main function of data collection system is to measure the capacitance value between the plates of measuring electrode, and then transmit the measured data set of capacitance values to the image reconstruction display section. Here, by applying appropriate image reconstruction algorithm to analyze the transmitted data set, the medium distribution in the measured pipe can be reconstructed. To be simple , the medium distribution of multi-phase flow is transformed into output capacitance value through the capacitance measuring sensor; then the capacitance value data is transmitted to image reconstruction display system through the data collection system; finally, reconstruct the medium distribution reconstruction image after analyzing the data through image reconstruction display system, thus achieving the goal of visualization.

Li Yan is the corresponding author.

2.2. Teaching Model of ECT Sensor

A The ECT sensor mainly includes three parts [15]: insulation pipe wall, measuring electrode and shielding layer. This paper will mainly study the system of 12-electrode ECT sensor. And the sensor's 12 plates are numbered from 1 to 12 accordingly. Any combination of two plates can form different electrode pairs, and in the pipe's cross section exists different measuring sensitive areas. Because each phase of the two-phase flow has different permittivity, the capacitance value of different electrode pairs on the ECT sensor will change when the components or flow pattern of two-phase flow in the pipe change. And the capacitance value statistics of all different electrode pairs will reflect the distribution of each phase in the whole cross section.

The capacitance value between any two plates can be showed as follows [18]:

$$C_{ij} = \iint \varepsilon(x,y) S_{ij}[(x,y),\varepsilon(x,y)] d_x d_y \tag{1}$$

Where C_{ij} refers to the capacitance value between electrode I and electrode j; $\varepsilon(x,y)$ is permittivity distribution function, $S_{ij}[(x,y),\varepsilon(x,y)]$ is distribution function of measuring sensitive areas.

2.3. SVM

SVM algorithm is put forward on the basis of optimal separating hyper-plane in the condition of linear separable.

This kind of separating hyper-plane can not only correctly classify all the training samples, but also make the distance from the point of all training samples which is the closest to separating hyper-plane to the separating hyper-plane reach the maximum.

Because of the maximum of classification interval, the complexity of classifier is under effective control, thus realizing better generalization ability of SVM. SVM shows its advantages in solving the problems of nonlinear separable. And through nonlinear transformation, SVM transforms the input space into a high dimensional feature space. And in this new space, we extract the optimal linear separating plane.

This paper applies the 12-electrode ECT system [16] [17], so the solved sample set is a column vector composed of 66 capacitance values and 66 sensitivity values. As the column of the samples matrix, this set is a nonlinear training set. And the sample space can be transformed into a high dimensional feature space through a nonlinear transformation, which makes the application of linear SVM algorithm in the high dimensional feature space possible and solves the high-dimension nonlinear classification problems in sample space.

SVM seeks for the optimal separating hyper-plane between any two things [9]. The given training sample set is $\{(x_i, y_i)\}_{i=1}^{n}, i = 1,2,...,n, x_i \in R^v$, where N is the sample number of training set, $y_i \in \{-1,+1\}$. The nonlinear original problem can be expressed as follows:

$$\begin{aligned} &\min_{w,b,\xi} \ \frac{1}{2}\omega^T\omega + c\sum_{i=1}^{l}\xi_i \\ &s.t \ \ y_i(\omega^T\phi(x_i)+b) \geq 1-\xi_i \\ &\quad \xi_i \geq 0, i = 1,...,l \end{aligned} \tag{2}$$

Where $\phi(x_i)$ refers to the mapping for the sample x_i from the input space into a high dimensional feature space; ω and b are undetermined hyper-plane parameters, respectively referring to normal vector and offset; $c > 0$ is penalty parameter for the

classification of samples; ξ_i is an introduced slack variable to solve nonlinear inseparable [10] [11] [12]. And equation(2) can be transformed to the dual problem:

$$\min_a \ \frac{1}{2}\sum_{i=1}^{l}\sum_{j=1}^{l}a_i a_j y_i y_j K(x_i,x_j)-\sum_{i=1}^{l}a_i$$
$$s.t\ \sum_{i=1}^{l}a_i y_i = 0, 0 \le a_i \le c, i = 1,...l \tag{3}$$

Where $K(x_i,x_j)=\phi(x_i)^T\phi(x_j)$ is kernel function. This paper applies RBF kernel function [13]:

$$K(x_i,x_j)=\exp(-\gamma \| x_i - x_j \|^2), \gamma > 0$$

The above equation can be transformed to the following:

$$K(x_i,x_j)=\exp(-(\int_0^{+\infty} x^{g-1}e^{-x}d_x)\| x_i - x_j \|^2) \tag{4}$$

Where g is the parameter of gamma kernel function, $g > 0$ is positive number。 Plug equation(4) into equation (3), we can get the optimal hyper-plane parameters ω and b_0 and Lagrange multipliers a^*.

The discrimination decision function of SVM is as follows:

$$t_r\_label = \mathrm{sgn}[\sum_{i=1}^{N} a_i^* y_i k(x_i,x) + b_0] \tag{5}$$

Where t_r_label is the decision result of unit r; x_i is the training set data namely the capacitance values and sensitivity values of ECT extracted from the finite element calculation.

3. Realization of FDRSVM Image Reconstruction Algorithm

3.1. Build a Model

In the experiment, the pipe's cross section of the ECT sensor model is first divided into 24 congruent fan-shaped units, then it is dealt with equal-area circle subdivision, so the pipe's cross section is divided into 24*8 fan-shaped units with equal area, that is to say, it is divided into 192 imaging units with equal area.

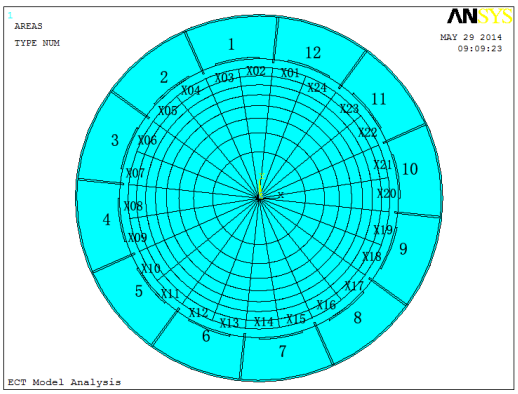

Figure 2. Model of ECT Subdivision Graph

In Figure 2, the pipe's cross section is circular and is divided into 8 layers from outside in, and each fan-shaped unit is numbered from X01 to X24 in counter-clockwise order, X=1, 2, …, 8, X refers to the layer number.

12 electrodes on the outside of the pipe are uniform-distribution, and they have the same parameter setting, namely, the parameters of the 12 electrodes are completely identical. The 12 electrodes can be mutually exchanged, and they have the feature of rotation symmetry. So we can conclude that the odd-numbered imaging units 1,3,5,…,23 have the feature of rotation symmetry, and the same with those even-numbered imaging units. Both the odd-numbered imaging units and the even-numbered imaging units have the feature of mirror symmetry. Because of this specialness, we can simplify the sample data set at a certain degree and remove the duplicate samples.

3.2. Feature Extraction and Feature Dimension Reduction

In order to facilitate the calculation, assume that the collected samples have been normalized. All the samples are divided into two parts, training samples and prediction samples:

1) $\mathrm{T}=\{(x_i, y_i)\}_{i=1}^{n}, i=1,2,...,n, x_i \in R^v, y_i \in \{-1,+1\}$

2) $\mathrm{D}=\{x_j\}_{j=1}^{m}, j=1,2,...,m, x_j \in R^v$.

where R^v is the vector space when v=132.

And we can simplify the training samples by the use of symmetry of the pipe's cross section, thus obtaining the following sample set without any repetition: $\mathrm{A}=\{(x_i, y_i)\}_{i=1}^{s}, i=1,2,...,s, s<n, x_i \in R^v, y_i \in \{-1,+1\}$ (the detailed process of simplification will be elaborated in the steps of algorithm).

By applying the method of clustering, the samples in set A are classified into several clustering sets which are different from each other. This paper will choose K-means clustering algorithm, because K-means algorithm [19] is not very complicated, and it is very suitable to deal with large sample data. K-means algorithm divides set A into K clusters, and $k<v$, all these clusters distinguish from each other. What can best represent the difference between cluster and cluster is the cluster center vector. Extract the center vector of each cluster. And all the central vectors can be seen as a group of linear independent feature vectors, namely, $d_1, d_2, ..., d_k$ (d_i is a 132-D feature vector, in which $i=1,2,...,k, k<s$), then we can get a column vector matrix $\mathrm{C}_{132\times k}=(d_1, d_2, ..., d_k)$, in which C can be regarded as a set of base in R^v. Based on linear transformation theory, the column vector matrix $\mathrm{A}_{s\times 132}=(\mathrm{x}_1,\mathrm{x}_2,...,\mathrm{x}_s)$ (In order to facilitate the calculation, the number y_i of each training sample is temporarily separated and independently form a new set $\mathrm{Y}=\{\mathrm{y}_i\}_{i=1}^{s}, i=1,2,...,s, y_i \in \{-1,+1\}$, thus making sure each y_i has a corresponding x_i)can be mapped from R^v to U^k, in which R^v, U^k respectively represent v-D linear space and k-D linear space in the real number field.

Having realized the transformation of A from R^v to U^k, we can get the image set A' of A in U^k. Any sample x_i in A will always have a corresponding sample x_i',namely:

$$\mathrm{F(A)}=\{x_i'=\mathrm{F}(x_i)|\ x_i \in \mathrm{A}, x_i' \in \mathrm{A}'\}, i=1,2,...,s, s<n$$

and we can find a linear transformation formula:

$$F(A)=AC=A'.$$

Where $A'_{s\times k}=(x'_1,x'_2,...x'_i),i=1,2,...,s,s<n$, the dimension number of each x'_i is k, $k<s$ and $k<v$.

Through the linear transformation, the training samples are transformed into a vector set with k-D vector space. The number of vectors which is *s* remains unchanged, while the dimension number is reduced from *v*-D to *k*-D, thus achieving the purpose of dimension reduction.

3.3. The Realization of FDRSVM Algorithm

Assume a certain imaging unit in the pipe is water, then the corresponding training result is 1; while if the imaging unit is oil, the corresponding training result is -1.

Step 1: Simplify the samples in training sample set T by the use of rotation symmetry and mirror symmetry. As shown in Figure 1, divide the pipe's cross section into n=24×8=192 units, and we can get n imaging units (the number of the imaging units is represented by n for the sake of generalization.) and 2^n combinations of water and oil distribution , namely 2^n samples. According to rotation symmetry, the actual samples without any repetition are as follows:

$$\left\lceil \frac{C_n^1}{24} \right\rceil+\left\lceil \frac{C_n^2}{24} \right\rceil+\cdots+\left\lceil \frac{C_n^n}{24} \right\rceil$$

so non-repetition sample set A is obtained.

Step 2: Calculate set A with K-means clustering algorithm, and we can get feature matrix $C_{132\times k}=(d_1,d_2,...,d_k)$.Then calculate A, C with linear transformation algorithm to get a new data set A', which has achieved the purpose of dimension reduction.

Step 3: Build SVM classification model with the new training sample set A', and choose penalty parameter c and kernel function parameter g. Then map the sample space into a high dimensional feature space through equation (4) RBF kernel function, plug equation (4) into formula(3) to get the optimal solutions a_i^* and b_0, to the original question. Finally, we can get the optimal training model after finishing training.

Step 4: Deal prediction samples D with feature dimension reduction before making the prediction, namely, $F(D)=DC=D_k$, then a new prediction sample set $D_k=\{x_j\}_{j=1}^m, j=1,2,...,m, x_j\in U^k$ can be obtained. Then plug it into equation (5) to make predictions of all units, and we can get n prediction results. Based on this, we reconstruct image.

4. Analyses of Experimental Results

For the sake of analysis, two groups of experiment are conducted. We make twice uniform divisions to the pipe's cross section, which are respectively 12-uniform-division and 24-uniform-division. And both have one layer. Then reconstruct image with SVM algorithm and FDRSVM algorithm respectively.

When the pipe wall is divided into 12 congruent units, the training data samples are 346 non-repetitive samples, and each sample is 132-D. Then randomly select 300 samples from the whole 212 samples to make prediction by applying SVM algorithm and FDRSVM algorithm respectively. Finally, make comparison and analysis of the results. As shown in Table 1:

Table 1. Prediction Error and Time of SVM Algorithm and FDRSVM Algorithm when Pipe is 12-Uniform-Division

Original figure	Average error		Prediction time (s)	
	SVM	FDRSVM	SVM	FDRSVM
Only one unit is oil	0.0633	0.0573	2.89	2.12
Only two units are oil	0.0647	0.0547	2.72	2.52
Only three units are oil	0.1129	0.1079	2.78	2.58

When the pipe wall is divided into 24 congruent units, the training data samples are 699059 non-repetitive samples, and each sample is 132-D. Then randomly select 300 samples from the whole 2^{24} samples to make prediction by applying SVM algorithm and FDRSVM algorithm respectively. Finally, make comparison and analysis of the results. As shown in Table 2:

Table 2. Prediction Error and Time of SVM Algorithm and FDRSVM Algorithm when Pipe is 12-Uniform-Division

Original figure	Average error		Prediction time (s)	
	SVM	FDRSVM	SVM	FDRSVM
Only one unit is oil	0.2073	0.0589	4.12	2.87
Only two units are oil	0.2547	0.0601	4.52	2.99
Only three units are oil	0.2879	0.1102	4.58	3.07

Seeing from Table 1 to Table 2, we can know that with the increase of training samples, the accuracy of image reconstruction becomes lower and the running time becomes longer when applying SVM algorithm alone. However, compared to SVM, FDRSVM algorithm has a better accuracy of image reconstruction and a shorter running time as the training samples increase.

Reconstruct images according to the prediction results, as shown in Table 3:

Table 3. Location Accuracy and Prediction Time of Image Construction

Original figure	Location accuracy	Prediction time	Reconstruct image
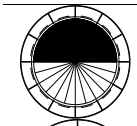	100%	0.21s	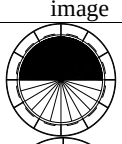
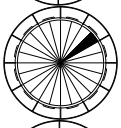	100%	0.13s	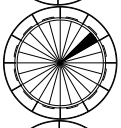
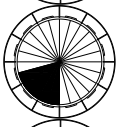	89.60%	0.52s	
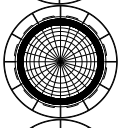	96.30%	2.32s	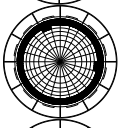
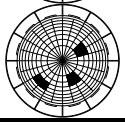	97.68%	2.69s	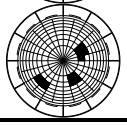

5. Conclusion

Aiming at the problems of long running time and low accuracy when using SVM to build classification model in ECT system with a large amount of sample set, this paper applies the method of dealing the training sample with feature extraction and dimension reduction, and it combines the rotation symmetry feature of ECT model to obtain high-quality training sample to build classification model. The above experimental results prove that applying FDRSVM to reconstruct image has a higher imaging accuracy and a shorter operating time in dealing with a large amount of sample data than applying SVM algorithm alone.

Acknowledgements

This study was supported by the Technology Innovation Talent Research Foundation of Harbin (No. 2013RFXXJ034), the National Natural Science Foundation of China (No.61103149),the Education Department Foundation of Heilongjiang Province(No.12521100) and the Natural Science Foundation of Heilongjiang Province(No. F2015038).

References

[1] L Haiqing, H Zhiyao, "Special detecting technology and application", M. Hangzhou：Zhejiang University Press, (**2000)**, pp. 72-82.
[2] Z Qiang, "Research on detective principle and methods of ECT/ERT dual-modal system", D. Tianjing: Tianjing university, (**2007)**, pp.1-17.
[3] U Datta, Dyakowski TS Mylvaganam. "Estimation of particulate velocity components in pneumatic Transport using pixel based correlation with dual plane ECT" , Chemical Engineering Journal, vol. 130, **(2007)**, pp. 87 - 99.
[4] Q Marashdeh oW Warsit, L S Fan, "Dual imaging modality of granular flow based on ECT sensors", J. Granular Matter, vol, 10, pp. 75 - 80 .
[5] Y TA, TN Phua, L Reichelt, "A miniature electrical capacitance tomography", J. Measurement Science and Technology, **vol.** 17, **(2006)**, pp. 2119-2129.
[6] C De-yun, C Yu, W Li-li, "A novel gauss-newton image reconstruction algorithm for electrical capacitance tomography system", Acta Electronica Sinica, vol. 3, no. 4,**(2009)**, pp. 739-743.
[7] Q Zhi-wei, H Yan, W Xue-ye, "Accelerate the filtering process of filtered back projection algorithm using fast hadamard transform", Journal of Electronics & Information Technology, vol. 32, no. 9, **(2010)**, pp. 2133-2138.
[8] Z Jinchuang, L Jinhua, L Zhigang, "Image reconstruction algorithm based on updated sensitivity field for ECT, J. Computer Engineering and Applications", vol. 48, no. 4, **(2012)**, pp. 167-169.
[9] VN. Vapnik , "Estimation of Dependencies Based on Empirical Data", Springer Verlag, **(1982)**.
[10] VN. Vapnik, "The Nature of Statistical Learning Theory", Springer, vol. 12, no. 9,**(1995)**.
[11] T. Devis, J. Marie, M. Kanevski, "Structured output SVM for remote sensing image classification", J.Journal of Signal Processing Systems, no. 35, **(2010)**, pp. 213-235.
[12] W De-cheng, LIN Hui. Imbalanced pattern classification method based on support vector machine and its application on fault diagnosis, J. Electric Machines and Control, no. 9, **(2012),** pp. 48-52.
[13] L Yan, Z Ping, C Jing, "Modified proximal support vector machine algorithm for dealing with unbalanced samples", J. Journal of Computer Applications, , vol. 34, no. 6, **(2014)**, pp. 1618-1621.
[14] L Hao-yang, C De-yun, L Mou-zun, "Image reconstruction algorithms of electrical capacitance tomography based on support vector machine", J. Harbin University of Science and Technology, vol. 11, no. 4, **(2006)**, pp. 1-4.
[15] L Yan, Y Xiaohua, L Jingsong, "Improved method of electrical capacitance tomography based on SVM algorithm of choice and segmentation", J. Computer Engineering and Applications, no**.** 5 **(2012)**,pp.1-8.
[16] W Q Yang, L H Peng, "Image reconstruction algorithms for electrical capacitance tomography Measurement", J. Science and Technology, (**2003) ,** no.14, pp. R1-R13.
[17] P Jiang, S Fan, T Xiong, "Investigation on the Sensitivity Distribution in Electrical Capacitance Tomography System", Indonesian J. of Electrical Engineering, vol.11, no. 12, **(2013)**, pp. 7088-7093.
[18] C De-yun, L Le-tian, H Hai-tao, "Image Reconstruction Algorithm Based on Iterated Tikhonov Regularization for Electrical Capacitance Tomography", Journal of Harbin University of Science and Technology, vol. 14, no. 2, **(2009)**.
[19] C Jun-jun, Y Liu-sen, L Peng, "Image Clustering via Combined Visual and Annotation Information", Journal of Harbin University of Science and Technology, vol. 19, no. 2, **(2014)**.

